Electromagnetic Field in the Neighborhood of the Focus of a Coherent Beam*

A. BOIVIN
Department of Physics, Laval University, Quebec, Canada
AND
E. WOLF
Department of Physics and Astronomy, University of Rochester, Rochester, New York
(Received 23 November 1964; revised manuscript received 17 February 1965)

An integral representation for the electromagnetic field in the region of focus of a coherent light beam that emerges from an aplanatic optical system has been derived by Ignatowsky (1919) and by Richards and Wolf (1959). In the present paper this representation is used to analyze the structure of the focal region in a typical case. Contours of the time-averaged electric energy density in the focal plane, in one defocused plane and in two meridional sections of the focal region of a system with angular semi-aperture 45° are presented. The meridional diagrams refer to axial sections through a cylindrical region around the axis near focus, of length 16λ and cross-sectional diameter 10λ, where λ is the wavelength of the light. It is found that the field has a strong longitudinal component at certain points of the focal plane and that longitudinal electric field strengths of the order of 10^5 V/cm could now be attained with focused laser beams. A diagram illustrating the complete behavior of the longitudinal component in the focal plane is also given.

1. INTRODUCTION

THE problem of determining the structure of the electromagnetic field in the region of focus of a coherent light beam has become of considerable interest, because of the possibility of producing very strong fields (of the order of several hundred thousands V/cm) by focusing the output of an optical maser. Such strong fields are being utilized, for example, for the generation of optical harmonics and for the study of high-energy scattering. It is evident that in order to utilize fully the potentialities promised by these developments, it is desirable to have some knowledge of the structure of the electromagnetic field in the focal region.

Early research on the structure of the focal region was based on the scalar-diffraction theory.[1] This work has proved very valuable in applications to instrumental optics. However, the results are not applicable to wide-aperture systems and, in any case, they do not exhibit vectorial features of the field, such as the state of polarization and the behavior of the Poynting vector. Investigations which take into account vectorial properties of the field are due to Ignatowsky,[2] Hopkins,[3] Burtin,[4] Focke[5] and Richards and Wolf.[6,7]

In this paper we present results of extensive computations relating to the field in the focal region of a monochromatic beam emerging from an aplanatic optical system. The computations are based on the vectorial integral representation of the field derived in Refs. 2 and 7. Some related results, both analytic and computational can also be found in these two references.

2. BASIC FORMULAS

Figure 1 illustrates the notation. The lens L represents an aplanatic system that converts the incident plane monochromatic wave into a converging spherical one, which is diffracted at the lens aperture. 2α is the angular aperture on the image side, i.e., the angle which the diameter of the lens subtends at the focus O, at distance f from the lens. OX, OY, OZ are Cartesian rectangular axes, with origin at the focus, with OX in the direction of vibration of the incident electric field, assumed to be linearly polarized, and with OZ along the axis of revolution, pointing away from the lens. (r,θ,ϕ) are spherical polar coordinates, with the polar axis along the axis of revolution of the system and with the azimuth $\phi=0$ in the OX direction.

Let

$$\mathbf{E}(P,t)=\mathrm{Re}\{\mathbf{e}(P)e^{-i\omega t}\},\quad \mathbf{H}(P,t)=\mathrm{Re}\{\mathbf{h}(P)e^{-i\omega t}\},\quad (1)$$

represent the electric and magnetic fields, respectively,

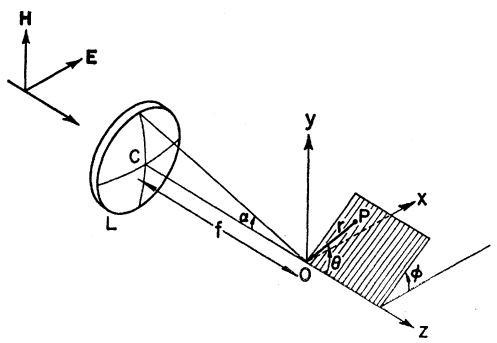

FIG. 1. Illustrating the notation.

* Research supported by the U. S. Army Research Office (Durham).

[1] For an account of this work see Sec. 8.8 in M. Born and E. Wolf, *Principles of Optics* (Pergamon Press, Inc., New York, 2nd ed., 1964).

[2] W. Ignatowsky, Trans. Opt. Inst. Petrograd (Leningrad) **1**, Paper IV (1919); **1**, Paper V (1920). See also V. A. Fock, *ibid.* **3**, 24 (1924).

[3] H. H. Hopkins, (a) Proc. Phys. Soc. **55**, 116 (1943); (b) Nature, **155**, 275 (1945).

[4] R. Burtin, Opt. Acta **3**, 104 (1956).

[5] J. Focke, Opt. Acta **4**, 124 (1957).

[6] B. Richards and E. Wolf, Proc. Phys. Soc. (London) **B69**, 854 (1956).

[7] B. Richards and E. Wolf, Proc. Roy. Soc. (London), **A253**, 358 (1959).

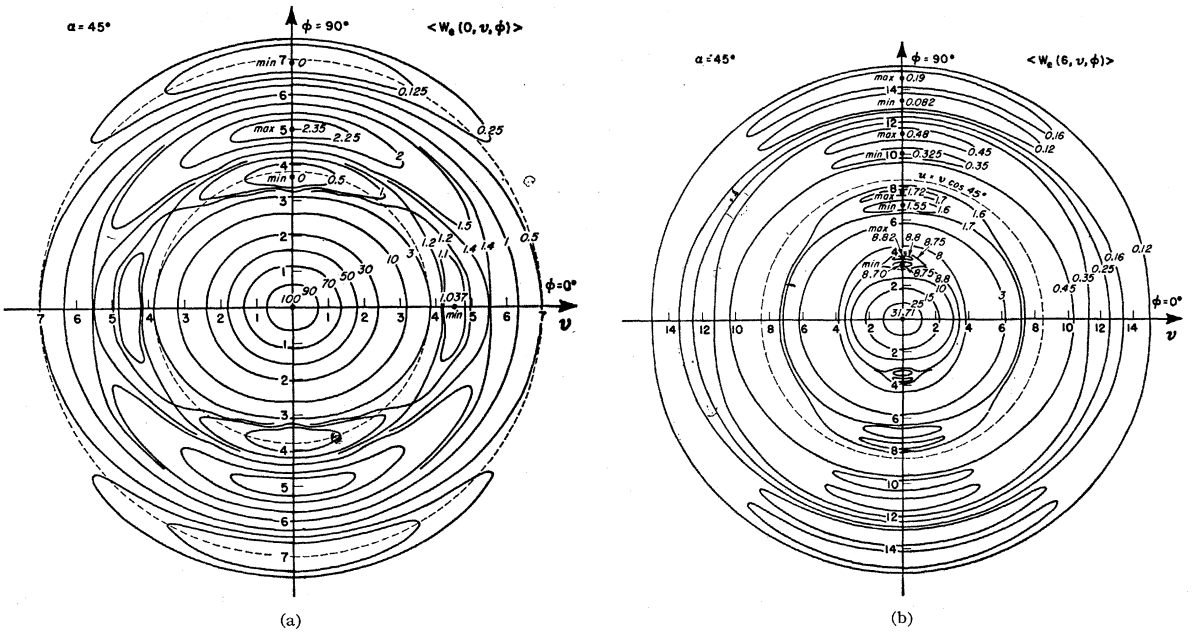

FIG. 2. Contours of the time-averaged electric energy density $\langle w_e \rangle$ in the focal plane $u=0$ (a) and in the plane $u=6$ (b), in a system with semi-angular aperture $\alpha=45°$ on the image side.

at a typical point P in the focal region, at time t, with Re denoting the real part. Then it has been shown in Ref. 7 that the Cartesian components of the space-dependent parts **e** and **h** of the electric and magnetic fields are given by[8] (in Gaussian units and with suitable choice of the origin of the phase)

$$\left.\begin{aligned} e_x(P) &= -iA(I_0+I_2\cos 2\phi), \\ e_y(P) &= -iAI_2\sin 2\phi, \\ e_z(P) &= -2AI_1\cos\phi, \end{aligned}\right\} \tag{2}$$

$$\left.\begin{aligned} h_x(P) &= -iAI_2\sin 2\phi, \\ h_y(P) &= -iA(I_0-I_2\cos 2\phi), \\ h_z(P) &= -2AI_1\sin\phi, \end{aligned}\right\} \tag{3}$$

where

$$\begin{aligned} I_0 \equiv I_0(kr,\theta;\alpha) &= \int_0^\alpha \cos^{1/2}\theta' \sin\theta'(1+\cos\theta') \\ &\quad \times J_0(kr\sin\theta'\sin\theta)e^{ikr\cos\theta'\cos\theta}d\theta', \\ I_1 \equiv I_1(kr,\theta;\alpha) &= \int_0^\alpha \cos^{1/2}\theta' \sin^2\theta' \\ &\quad \times J_1(kr\sin\theta'\sin\theta)e^{ikr\cos\theta'\cos\theta}d\theta', \end{aligned} \tag{4}$$

$$\begin{aligned} I_2 \equiv I_2(kr,\theta;\alpha) &= \int_0^\alpha \cos^{1/2}\theta' \sin\theta'(1-\cos\theta') \\ &\quad \times J_2(kr\sin\theta'\sin\theta)e^{ikr\cos\theta'\cos\theta}d\theta', \end{aligned}$$

and J_0, J_1, J_2 are Bessel functions of the first kind. The proportionality constant A in Eqs. (2) and (3) is given by

$$A=\pi fl/\lambda, \tag{5}$$

where l represents the amplitude of the incident electric field in the object space, f is the focal length of the lens, $\lambda=2\pi c/\omega$ is the wavelength, and c is the vacuum velocity of light.

It is of interest to note that according to Eq. (2) and (3) the electric and magnetic fields have in general nonvanishing "longitudinal" components (z-components) in the focal region.

It is convenient to introduce the following "longitudinal" and "transversal" coordinates of the typical point P in the region of focus (see Fig. 1):

$$\left.\begin{aligned} u &= kr\cos\theta\sin^2\alpha = kz\sin^2\alpha, \\ v &= kr\sin\theta\sin\alpha = k(x^2+y^2)^{1/2}\sin\alpha, \end{aligned}\right\} \tag{6}$$

where $k=2\pi/\lambda=\omega/c$. The position of P is then specified by the variables u, v, and ϕ. The three integrals defined by (4) now become functions of u, v (and of the parameter α which we will not show explicitly from now

[8] There are several misprints in Ref. 7. The last equation of (3.14) should read

$$\langle w(u,v,\phi)\rangle = (A^2/8\pi)\{|I_0|^2+4|I_1|^2+|I_2|^2\}.$$

Equation (3.19) should read

$$\langle w_e\rangle = \langle w_m\rangle = \tfrac{1}{2}\langle w\rangle = \left(\frac{A}{15}\right)^2 \frac{16}{\pi}[1-\tfrac{5}{8}(\cos^{3/2}\alpha)(1+\tfrac{3}{5}\cos\alpha)]^2.$$

Formula (3.22) should read

$$|\langle \mathbf{S}\rangle| = \frac{cA^2}{8\pi}\{(|I_0|^2-|I_2|^2)^2+4(\mathrm{Im}[I_1(I_2^*-I_0^*)])^2\}^{1/2}.$$

The designations of the vertical axes in Fig. 4 and 5 of Ref. 7 have been interchanged. The vertical axes in Figs. 4(a) and (4b) represent $\langle w_e(0,v,0)\rangle$ and $\langle w_e(0,v,\frac{1}{2}\pi)\rangle$, respectively; the vertical axes in figures 5(a) and 5(b) represent $\overline{\langle w(0,v,\phi)\rangle}$ and $\langle S_z(0,v,\phi)\rangle$, respectively.

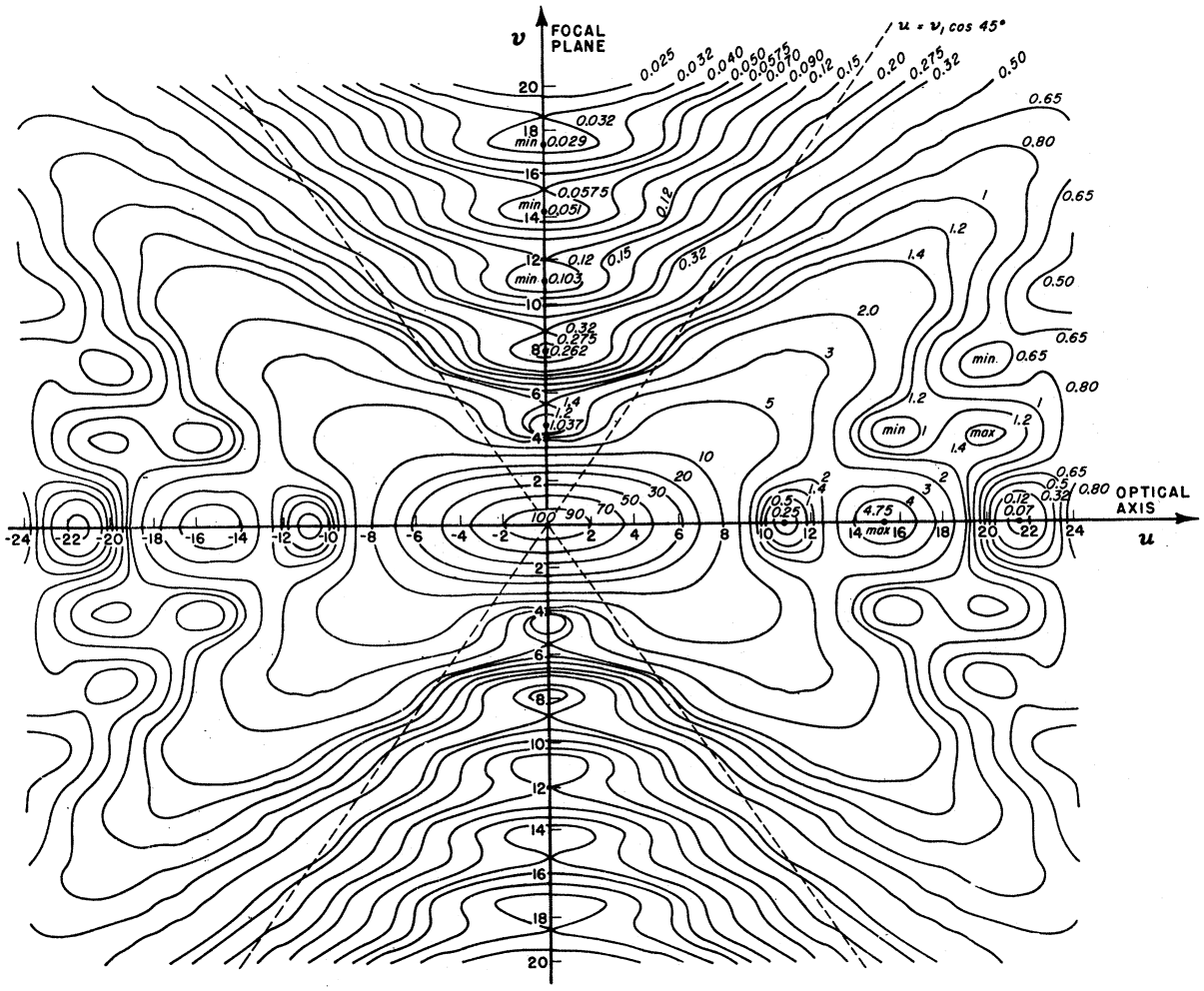

FIG. 3. Contours of the time-averaged electric energy density $\langle w_e \rangle$ near focus in the meridional plane $\phi=0$ ($\alpha=45°$).

on):

$$I_0(u,v)=\int_0^\alpha \cos^{1/2}\theta' \sin\theta'(1+\cos\theta') \times J_0\left(\frac{v\sin\theta'}{\sin\alpha}\right)e^{iu\cos\theta'/\sin^2\alpha}d\theta',$$

$$I_1(u,v)=\int_0^\alpha \cos^{1/2}\theta' \sin^2\theta' J_1\left(\frac{v\sin\theta'}{\sin\alpha}\right)e^{iu\cos\theta'/\sin^2\alpha}d\theta', \quad (7)$$

$$I_2(u,v)=\int_0^\alpha \cos^{1/2}\theta' \sin\theta'(1-\cos\theta') \times J_2\left(\frac{v\sin\theta'}{\sin\alpha}\right)e^{iu\cos\theta'/\sin^2\alpha}d\theta'.$$

3. RESULTS RELATING TO A TYPICAL CASE

The theoretical solution which was summarized in Sec. 2 was used to obtain detailed information about the structure of the focal region in an aplanatic system with angular semi-aperture $\alpha=45°$. First the values of the three integrals I_0, I_1, and I_2 were computed on an 7070 IBM electronic computer. The range covered was $0\leqslant u\leqslant 24$, $0\leqslant v\leqslant 20$ (in steps $\Delta u=0.25$, $\Delta v=0.5$) and corresponds, according to Eq. (6), to defocusing of amount $|z|\lesssim 8\lambda$ and to off-axis distance $r\lesssim 5\lambda$. With the help of these results and using graphical interpolation techniques, diagrams exhibiting the behavior of various quantities of physical interest were then constructed. The results are shown in Figs. 2–5. Each of the figures is normalized in such a way that at the focus, the time-averaged electric-energy density[9] $\langle w_e \rangle=100$, with

[9] To convert to actual values in physical units we use the results [cf. Ref. 7, Eqs. (2.28) and (3.17)] that at the focus

$$\langle w_e \rangle=\frac{1}{16\pi}\langle E^2\rangle=(A_G{}^2/16\pi)\,|I_0(0,0,\alpha)|^2 \quad \text{(Gaussian units)},$$

$$\langle w_e \rangle=\tfrac{1}{4}\langle E^2\rangle=\tfrac{1}{4}A_{mks}{}^2\,|I_0(0,0,\alpha)|^2 \quad \text{(mks units)},$$

where $A=\pi l f/\lambda$ and l is the strength of the linearly polarized electric field incident on the imaging system. In the present case ($\alpha=45°$), $I_0(0,0,\alpha)=0.5021$ and hence our normalization implies that we have taken

$$A_G=141.20 \text{ statV/cm},$$
$$A_{mks}=39.83 \text{ V/m}.$$

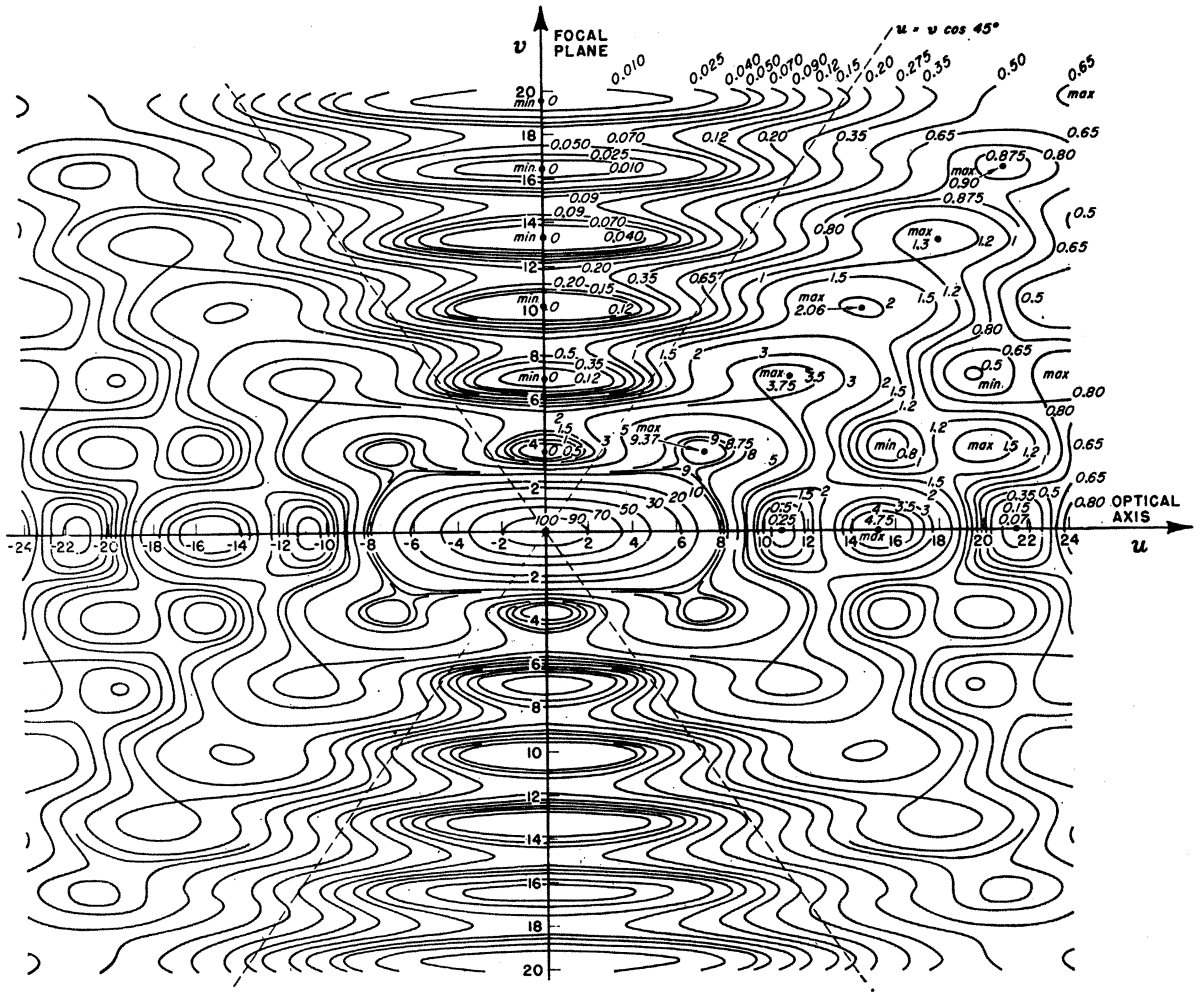

FIG. 4. Contours of the time-averaged electric energy density $\langle w_e \rangle$ near focus in the meridional plane $\phi=\frac{1}{2}\pi$ ($\alpha=45°$).

the definition (appropriate to Gaussian units) $\langle w_e \rangle = (1/8\pi)\langle E^2 \rangle = (1/16\pi)\mathbf{e}\cdot\mathbf{e}^*$ being used in labeling the contours in Fig. 5.

It is apparent from Figs. 2 that the contours of the electric-energy density $\langle w_e(u,v,\phi) \rangle$ in the observing planes $u=0$ and $u=6$ are not rotational symmetrical as the elementary scalar theory predicts (cf. Ref. 1, Sec. 8.5.2 and Sec. 8.8). However, they exhibit symmetry with respect to the two meridional planes $\phi=0$ and $\phi=\frac{1}{2}\pi$. In the focal plane ($u=0$) the contours, inside the central core, are approximately elliptical, with their major axes in the direction of the electric vector of the incident wave ($\phi=0$). Along the meridional line $\phi=\frac{1}{2}\pi$ in the focal plane there are points at which the electric-energy density has zero value. On the other hand, the minima along the meridional line $\phi=0$ are not zero. The contours of the time-averaged magnetic-energy density are obtained by simply rotating the contours of Figs. 2 through 90° about the normals to the plane of the figures, while keeping the u and v axes fixed.

Figures 3 and 4 show the contours of the time-averaged electric-energy density near the focus in the meridional planes $\phi=0$ (containing the electric vector of the incident field) and $\phi=\frac{1}{2}\pi$ (at right angles to the electric vector of the incident field).[10] In each figure the two dashed lines $u=v\cos 45°$ indicate the boundaries of the geometrical shadow. Along the optical axis, $v=0$, the minima are not true zeros and the distribution is compressed toward the focus in comparison with the corresponding distribution in systems with small angular aperture 2α. In both figures the alternate rows of minima and maxima are seen to be aligned along mutually parallel straight lines. In Fig. 4 the very complicated behavior in the "wings" of the pattern should be noted. These two diagrams show that linear polarization of the incident field leads to a distribution which in the plane $\phi=0$ is similar to that associated

[10] Figures 3 and 4 also represent the contours of the time-averaged magnetic energy density $\langle w_m \rangle$ near focus m, the meridional planes $\phi=\frac{1}{2}\pi$ and $\phi=0$, respectively ($\alpha=45°$).

with spherical aberration and in the plane $\phi=\frac{1}{2}\pi$ is similar to one associated with amplitude filtering.

Figure 5 shows the behavior of the longitudinal component (z-component) of the electric field in the focal plane $u=0$ or more precisely, the contours of e_z, the longitudinal component being given by $E_z=\mathrm{Re}(e_z e^{-i\omega t})$. The striking resemblance of this diagram to the well known instantaneous picture of the lines of force due to an oscillating electric dipole[11] should be noted.

While e_z is seen to be zero at the focus itself, and on the azimuthal line $\phi=\frac{1}{2}\pi$, it has maxima of alternative signs along the azimuthal line $\phi=0$, the largest one being attained at the point $v=2.25$ (about half a wavelength from the axis) in the azimuth $\phi=0$. This maximum is about 27.9% of the maximum value which the transverse component attains (at the focus itself). At the points $v=3.98, 7.10, 10.24, 13.45, \cdots$ on the line $\phi=0$ the transverse electric field is strictly zero, so that at these points the electric field is *purely longitudinal*. The values of the e_z component at these points are: $e_z=-9.70, +4.70, -2.80, +1.85, \cdots$. With the help of these results one can readily see that by focusing a beam emerging from an optical maser, longitudinal field strengths of the order of 10^5 V/cm can now be attained. It seems plausible that such strong longitudinal fields could be used for accelerating charged particles. However, because of the considerable complexity of the field in the focal region, the practical feasibility of such a proposal must await a more detailed study. In any case it should be born in mind that the present calculations refer to a wave whose amplitude distribution on emergence from the lens is that appropriate to aplanatism [see Ref. 7, Eq. (2.13)], whereas the amplitude distribution of a laser beam will be of a more complicated structure. One could, of course, employ a suitable "amplitude filter" to convert the laser output distribution into an aplanatic one.

[11] See, for example, G. Joos, *Theoretical Physics* (Blackie & Son Ltd., London, 1947), p. 327.

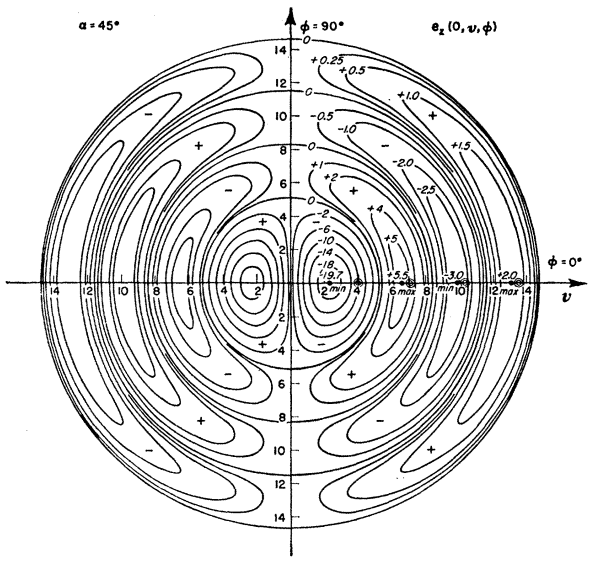

FIG. 5. Contours of the time-independent part e_z associated with the longitudinal component of the complex electric field $E_z=\mathrm{Re}\{e_z e^{-i\omega t}\}$ in the focal plane $u=0$ ($\alpha=45°$).

An extensive computational program is at present in progress and it is expected that it will provide detailed information about the longitudinal and transverse components of the field and about the Poynting vector in the focal region.

ACKNOWLEDGMENTS

We are indebted to Mrs. C. Reynolds for much advice and help with programming and to Mrs. G. Eyer for considerable assistance with the preparation of the figures. We also wish to acknowledge some help received from J. Dow in connection with the computations. Further, one of us (A.B.) is indebted to the John Simon Guggenheim Memorial Foundation for the award of a Fellowship, during the tenure of which the largest part of this work was carried out.